Adsorption of Methanol on the MgO(100) Surface: An Infrared Study at Room Temperature

Jennifer Rudberg and Michelle Foster*

Department of Chemistry, University of Massachusetts-Boston, 100 Morrissey Boulevard, Boston, Massachusetts 02125

Received: July 14, 2004; In Final Form: September 15, 2004

Methanol adsorbed on the (100) face of MgO has been studied at room temperature and elevated methanol pressures using transmission Fourier transform infrared spectroscopy. From these investigations, we find evidence of two structures for the adsorbed methanol. At low coverages, the methanol molecules congregate into two-dimensional islands that are strongly associated with the substrate. The properties of this submonolayer-to-monolayer thin film are similar to those of solid methanol. Once the available surface sites are occupied and a complete monolayer has formed, the methanol begins to condense in multilayers, creating a thin film on the surface with properties similar to liquid methanol.

Introduction

Magnesium oxide is often described as a model basic oxide, having a simple rock salt structure, a single valence state, and only one stable low-index surface orientation: the (100) face. MgO has been shown to catalyze the hydrogenation of 1,3-butadiene, the H_2 and D_2 exchange reaction, and the dehydrogenation of methanol and formic acid.[1] As such, it is well suited to fundamental studies of adsorption and catalysis at oxide surfaces. The surface chemistry and physics of metal oxides, and the characterization of adsorbates on these materials, are important to many natural and industrial processes.[2,3] Despite the evident need, few surface spectroscopic studies have been reported on well-characterized mineral surfaces. Such studies have been hampered by the inherent complexity of oxide surfaces and the experimental difficulty of using electron and ion spectroscopies for the analysis of insulating materials. As a result, although they are essential for a more complete understanding of reactions on oxide surfaces at the molecular level, studies using a surface science approach are limited, and the investigation of magnesium oxide adsorption systems has been confined, in general, to the less well-defined surfaces of powders.[4–6] To avoid the problems associated with analysis of single-crystal samples of an insulating material, a number of studies have made use of thin films of well-characterized MgO-(100) grown on a conducting substrate, typically either Mo(100)[7–10] or Mg(0001).[11,12] However, the use of optically based spectroscopy such as transmission infrared (IR) spectroscopy avoids the use of charged particles altogether.[13,14]

The adsorption of methanol on magnesium oxide has been investigated on powder samples, well-characterized thin films, and single-crystal substrates.[4–6,15] The interaction of methanol with magnesium oxide powders has been studied with IR spectroscopy,[4,6] temperature-programmed desorption (TPD) mass spectrometry,[5] and nuclear magnetic resonance (NMR) spectroscopy[15] to show four distinct species on the surface: methanol physisorbed to the substrate, methanol chemisorbed to the substrate through a hydrogen bond to the oxygen ion in the surface, and two reacted methoxy species. The first reacted species is bonded by a monodentate linkage through an oxygen atom to a magnesium ion, with an adjacent hydrogen atom forming a hydroxyl group with an exposed oxygen ion of the surface, resulting from the breaking of the O–H bond in the adsorbed methanol. The second reacted species is bonded through a bidentate linkage via the methanol oxygen atom to two magnesium ions on the substrate. Recent theoretical investigations of methanol on MgO support these assignments.[7,16,17]

Under typical ultrahigh vacuum (UHV) conditions at both cryogenic temperatures[7–12] and room temperature,[11,12] methanol adsorption has also been studied on thin films of MgO(100) by exposing the substrate to a known pressure or coverage of methanol and then reestablishing UHV before examining the surface. For this reason, only the cryogenic studies showed any type of physisorption between the methanol and the MgO(100) surface with methanol wetting the surface and growth occurring in layers, that is, the methanol monolayer is saturated before multilayer formation begins.[8,18] Any reaction occurring on the thin film MgO(100) substrate has been linked to defect sites such as terrace steps, edges, and vacancies on the surface.[7,11,12] When reactions were seen between methanol and the thin films of MgO(100), they occurred through cleavage of the O–H bond in the methanol, forming a surface methoxide species similar to the monodentate linkage described above on MgO powders.[7–12]

Few studies have been performed to investigate methanol adsorption on single-crystal MgO(100) substrates, and they were always under UHV conditions.[11,12] These investigations concur with those on the thin films of MgO(100) in that the atomically smooth terraces show no reaction with methanol. Only when the substrate has been intentionally damaged by sputtering is limited reactivity seen between methanol and the MgO(100) surface. It is important to reiterate that these studies were performed under UHV, nonequilibrium conditions and, until now, no studies have been performed under ambient conditions on the dynamic equilibrium occurring between methanol in the gas phase and the single-crystal MgO(100) surface.

* To whom correspondence should be addressed. Telephone: 1-617-287-6096. FAX: 1-617-287-6066. E-mail: michelle.foster@umb.edu.

This paper describes a study that uses transmission Fourier transform infrared (FTIR) spectroscopy to study methanol on MgO(100) at room temperature and methanol pressures ranging from 0.1 Torr up to 105 Torr. In this manner, it is possible to investigate the surface interactions of adsorbed methanol in dynamic equilibrium with the gas phase on the MgO surface. Frequency shifts, bandwidths, and absorbance values of the OH stretching features are used to interpret the structure and phase of the interfacial region, giving both a qualitative and a quantitative understanding of methanol adlayers.

Experimental Section

For spectroscopic measurements, 16 crystals, cleaved along the (100) faces of MgO (MTI Corporation) under dry nitrogen purge, were placed in a cylindrical stainless steel sample cell that has been described elsewhere.[19,20] Spacers made of 0.1 mm diameter Ta wire were sandwiched between the crystals so that the MgO faces did not touch. Calcium fluoride windows (Infrared Optical Products, Inc.) were attached to both ends of the cell and then sealed with Viton O-rings.

The cell was attached to a vacuum line and then pumped with a diffusion pump to a base pressure of 10^{-6} Torr. The cell and line were baked under vacuum at 110 °C for 2 days to remove contaminants. The methanol vapor was obtained from a liquid sample (Aldrich, HPLC grade) and further purified by a number of freeze−pump−thaw cycles. Methanol vapor was introduced at the desired pressure, and the dynamic equilibrium occurring between the methanol and the MgO(100) surfaces was monitored by transmission FTIR spectroscopy (Nicolet, Nexus 670) using 8 cm^{-1} resolution. An InSb detector was used during these studies that, coupled with the CaF$_2$ windows, limits the frequency range of the FTIR spectra collected to 4500−1800 cm^{-1}.

The MgO crystals were monitored, using transmission FTIR spectroscopy, for the presence of carbonaceous contamination in the form of a C−H stretch at ∼3000 cm^{-1} (ref 21) and a C=O stretch at ∼2200 cm^{-1} (ref 22). Concurrent studies using identically prepared crystals in a different cell and using ZnSe windows and an MCT detector allowed for the inspection of the crystals for the suspected reaction between MgO and CO$_2$ to form MgCO$_3$ by probing the spectra for the carbonate features, bands centered at 1660 and 1310 cm^{-1} (ref 23). At no time during this series of experiments were any carbon-containing features seen in any of the IR spectra. This is predictable in light of recent experiments on single-crystal MgO, indicating that any reaction occurring between MgO(100) and CO$_2$ is reversible.[24] These results indicate that it is very unlikely that the surfaces of the crystals used in these experiments are contaminated with carbonaceous compounds.

For the methanol vapor spectroscopic investigations, a second sample cell was built using a quartz body[25] press-fit against windows of ZnSe (Infrared Optical Products, Inc.), once again using Viton O-rings as the sealing medium. The combination of the MCT detector and the ZnSe windows allows the FTIR spectra to access a frequency range of 4000−800 cm^{-1}. The methanol vapor was introduced into the cell by a method identical to the one described for the adsorption studies.

The ATR-FTIR spectra of liquid methanol (Aldrich, HPLC Grade) were taken by using a Nicolet Avatar spectrometer with a room-temperature DGTS detector and a germanium-window, single-bounce, attenuated total reflectance (ATR) accessory (Nicolet Omni Sampler) installed into the sample compartment.
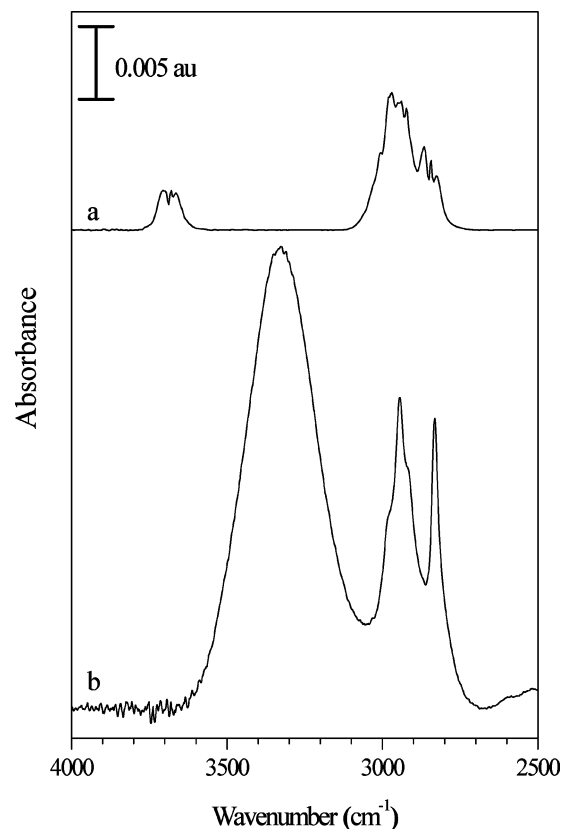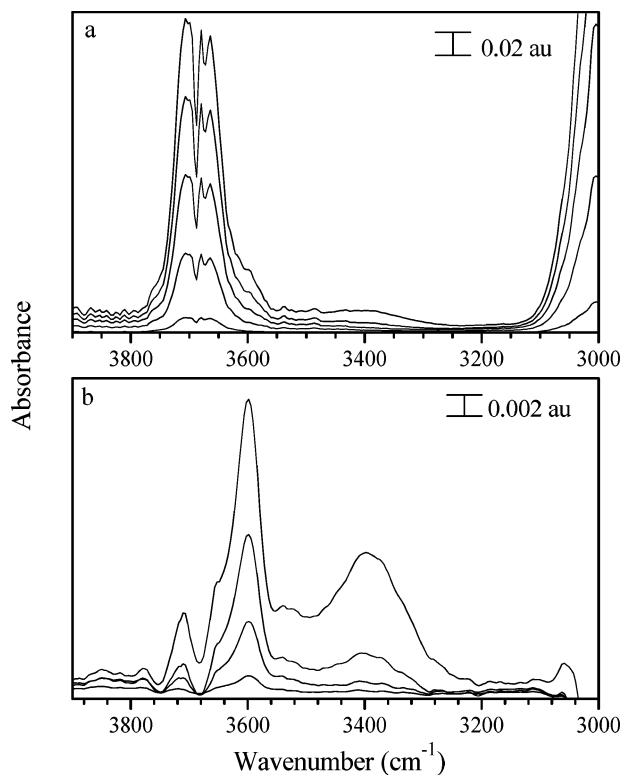

Figure 1. (a) FTIR spectra of 1.04-Torr methanol vapor and (b) ATR-FTIR spectra of pure methanol liquid. Both spectra are sampling identical number densities of methanol, 1.7×10^{17} molecules/cm^2.

Results and Discussion

1. Methanol Vapor. The OH stretch of methanol in an IR spectrum shifts according to the phase and hydrogen-bonding arrangement. Figure 1 shows the infrared absorption spectra of 1.04-Torr methanol vapor (top) and that of a drop of liquid methanol on the ATR crystal (bottom). The number of molecules examined for each of these spectra is nearly identical at 1.7×10^{17} molecules/cm^2. The OH stretch appears at 3700 cm^{-1} for the vapor phase, while in the condensed phase the OH stretching feature is enhanced by a factor of 10 and red-shifted 350 cm^{-1} to approximately 3350 cm^{-1} as a function of the hydrogen bonding and condensation. The CH stretching features remain virtually unchanged at 2950 and 2830 cm^{-1}, with a doubling of the intensity because of the condensation of methanol.

Methanol is very much like water in that its physical state, and thus the extent and the rigidity of its hydrogen bonding, can be investigated with FTIR spectroscopy. In previous studies, while investigating the interactions between water and MgO(100),[19] the water vapor features in the FTIR spectra of water thin films on MgO(100) could be removed via subtraction using a reference water vapor spectrum. This procedure is possible because the OH stretching feature in the FTIR spectrum of water vapor does not vary as a function of pressure under ambient conditions (the vapor pressure of water is 17.6 Torr at 20 °C). This is not true of methanol vapor. The vapor pressure of methanol at ambient temperatures is an order of magnitude greater than that of water, 110 Torr at 22 °C, and there are slight changes occurring in the spectra as a function of pressure. This can be seen in Figure 2a, which shows the OH stretching region for methanol vapor at pressures of 5, 25, 50, 75, and 100 Torr. This region of the spectrum is dominated by the monomer gas-phase features with its OH stretch appearing at

Adsorption of Methanol on MgO(100)

*J. Phys. Chem. B, Vol. 108, No. 47, 2004* **18313**

Figure 2. (a) FTIR spectra of methanol vapor at 5, 25, 50, 75, and 100 Torr (from bottom to top). (b) Gas-phase hydrogen bonding in methanol vapor, obtained by the subtraction of FTIR spectrum of 5-Torr methanol from spectra at 25, 50, 75, and 100 Torr (from bottom to top).


Figure 3. (a) Concentration of methanol molecules hydrogen bonding in the gas phase as a function of methanol pressure, calculated as described in the text. (b) The number of methanol molecules undergoing hydrogen bonding presented as a percentage of the total number of methanol molecules present.

$\sim$3700 cm^{-1}. However, there are also features appearing at lower wavelengths, a shoulder at 3600 cm^{-1} and a peak at 3400 cm^{-1}, that cannot be explained by noninteracting gas-phase methanol molecules.

The spectra in Figure 2b have been modified using a 5-Torr methanol vapor spectra to subtract out the monomer features, leaving only the peaks that may be attributed to hydrogen-bonded methanol vapor. These features have been assigned in a recent investigation by Dixon et al.[26] Using ab initio calculations and comparisons with dilute liquid solutions, the peak at 3600 cm^{-1} was assigned to an open methanol dimer, while the feature seen at 3400 cm^{-1} was due to higher-order methanol polymers, probably trimers and/or tetramers in a cyclic configuration. No attempt was made to quantify the hydrogen-bonded methanol.

The quartz cell used for the methanol vapor studies has a known path length (5.00 ± 0.05 cm), and using this value in a Beer's Law calculation, along with the integrated areas of both the non-hydrogen-bonding OH peak at $\sim$3700 cm^{-1} and the CH feature centered at 2900 cm^{-1} for a number of methanol vapor FTIR spectra at pressures lower than 5 Torr, values were calculated for the molecular cross sections for methanol using these two features. For the CH stretching region (integrated from 2725 to 3140 cm^{-1}) the molecular cross section, $\bar{\sigma}_{g,CH}$, was calculated to be 9.7×10^{-18} cm/molecule. For the monomeric OH stretching region (assuming there is minimal hydrogen bonding occurring in the gas phase at these low pressures) integrated from 3560 to 3780 cm^{-1}, the molecular cross section, $\bar{\sigma}_{g,OH}$, was calculated to be 1.6×10^{-18} cm/molecule. These values were then used to calculate the concentration of the methanol vapor present at pressures up to 105 Torr. The difference between the methanol concentrations calculated from the CH stretch (the actual methanol concentration) and the OH
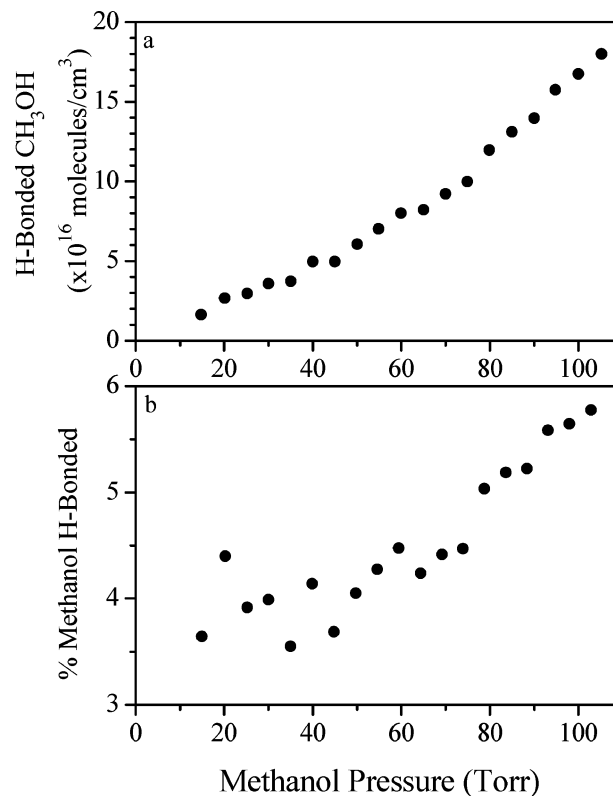
monomeric stretch (the concentration of methanol monomers) gives a rough estimate of the concentration of methanol molecules undergoing hydrogen bonding.

This concentration of hydrogen-bonded methanol molecules as a function of total methanol pressure is presented in Figure 3a. If the hydrogen-bonding arrangement in the gas phase is the same as that calculated by Dixon et al.,[26] namely an open dimer and cyclic tetramer, then the concentration of methanol monomers calculated from the integrated area of the feature at 3700 cm^{-1} includes both true monomers and one-half of every dimer pair, and thus is a high estimate. This means that the calculated value of the concentration of molecules hydrogen bonding in the gas phase is a low estimate. Attempts to use these data to calculate the concentration of methanol dimers versus the molecules hydrogen bonding in larger clusters have been unsuccessful, since the two configurations of hydrogen-bonded clusters have led to drastically different molecular cross sections for the OH stretch.

Figure 3b presents this same calculation in terms of the percentage of molecules participating in hydrogen bonding, the ratio of the difference between methanol concentrations calculated using the CH stretch peak, and the OH stretch feature with respect to the total concentration of methanol present, multiplied by 100. It is interesting to note that at pressures below 55 Torr, the percent of hydrogen-bonded methanol molecules is fairly constant at about 4% with a slight increase with increasing pressure; yet, at methanol pressures of 60 Torr up to 105 Torr, there is a notable increase in the percentage of hydrogen-bonded methanol.

This fact is very important in the current study, which investigates the interactions occurring between the MgO(100) surface and many different pressures of methanol vapor during
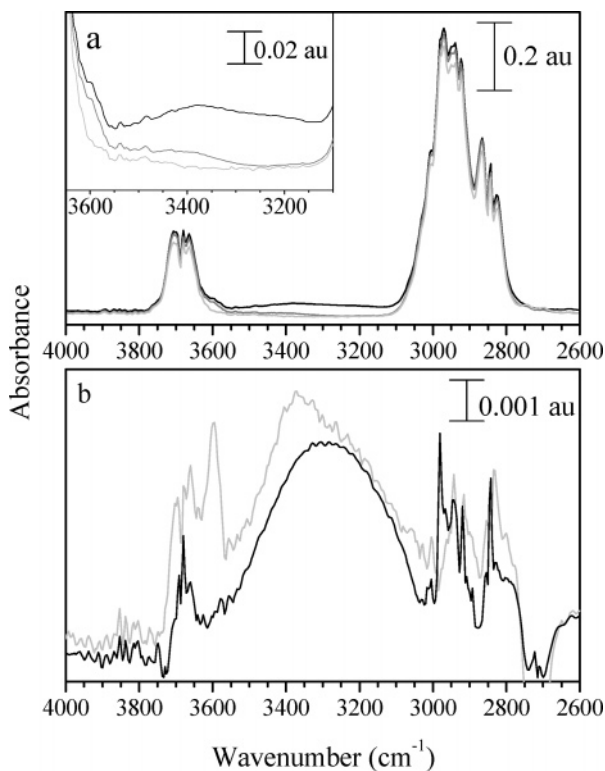
Figure 4. (a) FTIR spectra of 5-Torr methanol vapor (light-gray spectrum on bottom, ×17), 90-Torr methanol vapor (dark-gray spectrum in middle), and 90-Torr methanol in equilibrium with 16 MgO(100) crystals (black spectrum on top, ×5). (Inset) Enlarged view of the hydrogen-bonded OH stretching region of the same three spectra. (b) Subtraction result of 90-Torr methanol in association with MgO(100), $n = 32$, using both the 90-Torr methanol vapor spectrum (black) and the 5-Torr methanol spectrum (light gray) as a reference spectra for removal of the vapor features.

dynamic equilibrium. The presence of hydrogen bonding in the FTIR spectrum is not enough to distinguish between methanol in the vapor phase and methanol condensed on our substrate. When investigating the interaction between a model surface and any molecule at elevated pressures, extensive knowledge of how that molecule behaves when the substrate is absent is essential.

2. Methanol and Magnesium Oxide. The experimental apparatus used for this study has been designed to minimize the number of molecules in the gas phase probed during our adsorption studies. However, even with these extreme measures, the signal from the gas-phase methanol drowns out the signal from adsorbed methanol, as can be clearly seen in Figure 4a; the black spectrum is that of 90 Torr of methanol in the presence of 16 MgO(100) crystals. The adsorbed methanol is represented by the slight mound appearing in this spectrum at approximately 3300 cm^{-1}. However, because of the residual gas-phase methanol in the sample cell, it is difficult to quantify this adsorbed feature. The residual gas-phase features can be subtracted out of this spectrum, leaving only those features representative of the adsorbed methanol adlayer. Typically in this type of investigation,[19,27−31] a low-pressure, vapor-phase reference spectrum is chosen and used to subtract the vapor features from all the resulting sample spectra. For instance, the 5-Torr spectrum, shown in light gray in Figure 4a, could be used to remove the vapor features from the 90-Torr MeOH/MgO(100) sample spectrum, resulting in the light-gray adsorption spectrum shown in Figure 4b. However, because of the hydrogen bonding of methanol in the vapor phase, the resulting subtraction spectrum shows not only the features associated with methanol adsorbed to MgO(100) when at equilibrium with the

vapor but also the hydrogen bonding occurring in the gas phase, as indicated by the sharp feature at 3600 cm^{-1} and the asymmetry of the adsorbed feature culminating in a peak at 3400 cm^{-1}. By comparing this subtraction result with the spectra in Figure 2b, it is clear that these two features are due to methanol vapor.

Figure 4a also shows the gas-phase FTIR spectrum of 90 Torr of methanol, indicated in dark gray. In the full-scale versions of all three spectra, it is difficult to see any differences, but the inset shows the hydrogen-bonding region for all three spectra, 5-Torr methanol vapor, 90-Torr methanol vapor, and 90-Torr methanol vapor in the presence of 16 MgO crystals. In this expanded graph, it is easy to see the differences and similarities of the three spectra, most notably a shoulder at 3600 cm^{-1} and the feature at 3400 cm^{-1}, which are absent in the 5-Torr methanol vapor spectrum. When the 90-Torr methanol vapor spectrum is used as a reference for the subtraction of the vapor features from the spectrum of 90-Torr methanol in equilibrium with the MgO(100) surfaces, the black spectrum in Figure 4b is the result. The peak associated with the CH stretches can be seen between 2750 and 3050 cm^{-1}; these features are due to both adsorbed methyl groups on the surface and subtraction artifacts. Likewise, the feature centered at 3690 cm^{-1} is most likely due to gas-phase methanol and a result of poor subtraction; however, it could also be due to either non-hydrogen-bonded adsorbed methanol or the reversible dissociation of methanol on the surface. The peak of interest is the very broad feature, with a full width at half-maximum (fwhm) of 400 cm^{-1}, centered at 3300 cm^{-1}. This feature, which strongly resembles that of liquid methanol, is the OH stretching vibration of methanol adsorbed on MgO(100).

Absorption spectra of methanol adsorbed to MgO(100) at room temperature for a variety of pressures are shown in Figure 5. The bands are all broad, and the fwhm slightly decreases with increasing pressure, from a value of 460 cm^{-1} at 5 Torr to 390 cm^{-1} at 105 Torr. The peak center of the OH stretching feature of the adsorbed methanol also shifts as a function of coverage. At the lower pressures, the peak center is relatively constant at 3260 ± 10 cm^{-1}; but beginning at approximately 70 Torr, the peak center becomes increasingly blue-shifted until, at 105 Torr, the highest pressure investigated in this study, the peak center occurs at 3330 cm^{-1}. Figure 6 shows this peak shift trend as a function of methanol vapor pressure. The low-pressure methanol peak centers are close to the peak center seen for vitreous solid methanol cooled to −180 °C; this feature has been observed at 3235 cm^{-1} (ref 32). At approximately 70 Torr, the peak center begins to shift toward the 3337 cm^{-1} observed for bulk liquid methanol.[32] This seems to indicate that, at the lower pressures, the molecules are oriented in such a way that their hydrogen-bonding network is more solidlike; whereas as the pressure increases, the intermolecular interactions become decidedly more liquidlike.

Since the high-pressure absorption resembles that of bulk liquid methanol, its optical properties were used to estimate adlayer coverage. By making use of a modified Beer−Lambert relationship,[33,34] the integrated absorbance of a surface species is described by the following equation:

$$\bar{A} = \frac{n\bar{\sigma}S_{CH_3OH}}{2.303}$$

The integrated absorbance, $\bar{A}$ (cm^{-1}), of the adsorbed methanol was determined by numerical integration over the frequency range 3630−3030 cm^{-1}, S_{CH_3OH} is the surface density of
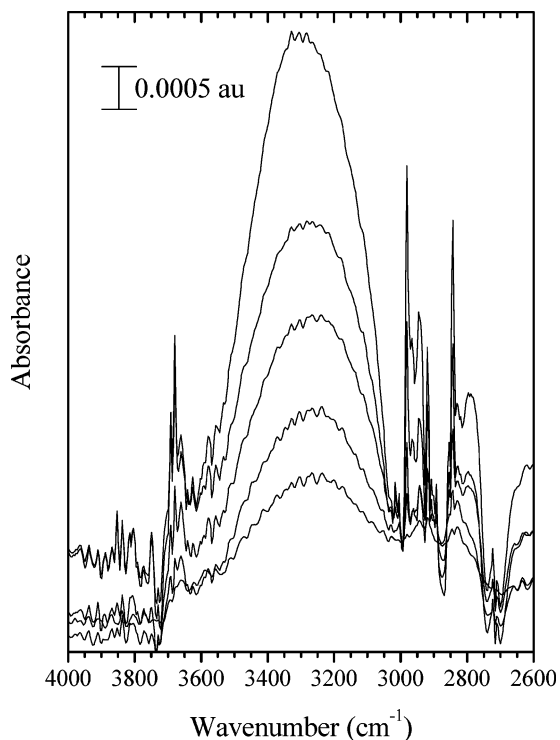
Figure 5. Absorption spectra of 5, 25, 50, 75, and 100 Torr (from bottom to top) of methanol adsorbed on MgO(100) at room temperature. These spectra correspond, respectively, to 0.45, 0.70, 0.90, 1.05, and 1.50 monolayers of methanol adsorbed to the MgO(100) surface. The number of MgO(100) crystal faces for these experiments is $n = 32$. Gas-phase features have been removed from these spectra by using the corresponding pressure of methanol vapor spectrum.
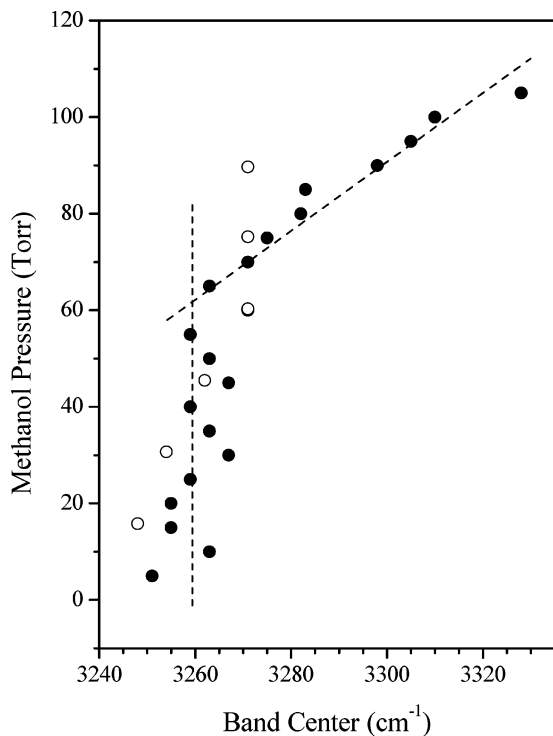
Figure 6. Band center change as a function of methanol pressure in equilibrium with MgO(100) at room temperature. Data taken on ascending and descending pressures are given by the closed and open circles, respectively. The lines are merely a guide for the eye.

adsorbed methanol, and n is the number of exposed MgO(100) faces, 32 for this series of experiments. The integrated cross section, $\bar{\sigma}$ (cm/molecule), was determined from the measured,

frequency-dependent, imaginary component, κ, of the index of refraction of bulk methanol[35] using:[36]

$$\bar{\sigma} = \left(\frac{4\pi}{\rho}\right)\int_{\text{band}}\kappa\tilde{\nu}\,\mathrm{d}\tilde{\nu}$$

where ρ is the molecular density of methanol at the given temperature. For methanol at room temperature, $\bar{\sigma}$ was found to be 1.02×10^{-16} cm/molecule. Once $S_{\text{CH}_3\text{OH}}$ is calculated, the coverage, $\Theta = S_{\text{CH}_3\text{OH}}/S_{\text{MgO}}$, is easily determined since S_{MgO} for the MgO(100) face is 1.13×10^{15} surface ions/cm^2 (ref 37). Using this procedure, all integrated absorbances are converted to coverages, Θ, in terms of methanol molecules per surface ion. Using this method of analysis, the methanol adlayer shown in Figure 4b corresponds to a coverage of 1.3 monolayers.

While we can justify the use of liquid methanol optical constants to calculate coverages when the band profiles of the bulk liquid and adlayers are similar, there is a systematic error introduced when the profiles differ as they do in the lower coverage features, which we shall associate with the submonolayer adlayer. It would be useful to make use of the optical properties of solid methanol for the low-pressure regime; however, those proved difficult to find in the literature, and thus, all calculations were made using the optical constants of liquid methanol. By comparing the properties of water, whose optical constants are very well represented in the literature,[38-40] with those of methanol, an estimation of the error associated with our calculations might be possible. The optical qualities of methanol and water are similar upon transition from the vapor to the liquid phase, namely, the myriad rotational−vibrational features of the gas transform into a single diffuse absorption band with a corresponding increase by a factor of 10 in the oscillator strength of the OH bond because of the hydrogen bonding within the system.[35,41] Therefore, perhaps the optical qualities of water during the liquid-to-solid transition may be used as a guide; liquid water has a peak center at 3400 cm^{-1} (ref 39), which shifts to 3250 cm^{-1} (ref 40) upon condensation to ice, while the oscillator strength of the OH stretch doubles. In correlations between the integrated cross section and band center for hydrogen-bonding systems just reviewed, we anticipate higher values of $\bar{\sigma}$ for the lower vibrational frequency of the low-coverage region, and thus, calculated coverage values are most likely underestimated by as much as 50%.

Isotherms may be determined from the pressure-dependent adlayer spectra through the photometry analysis just described. By using the spectra shown in Figure 5 and others as well, the room temperature adsorption isotherm for methanol on MgO(100) was calculated and is shown in Figure 7. The methanol coverage is plotted as a function of the methanol pressure at equilibrium within the cell. In this figure, the closed circles represent adsorption measurements, and the open circles are the desorption measurements. The highest pressure used in this series of experiments was 105 Torr. There is significant hysteresis shown in the isotherm. This hysteresis is not permanent, and the substrate is returned to virtually its initial state after being evacuated overnight. The reactivity between methanol and MgO(100) at high pressures and room temperature was recently investigated by this researcher using atomic force microscopy, and there were no topographical changes recorded when MgO(100) was allowed to sit in an atmosphere of pure methanol vapor for 100 h.[20]

According to the adsorption isotherm presented in Figure 7, a monolayer of methanol on MgO(100) occurs at a pressure of 70 Torr. We have defined one monolayer as a single methanol molecule adsorbed onto every available surface ion, both Mg^{2+}
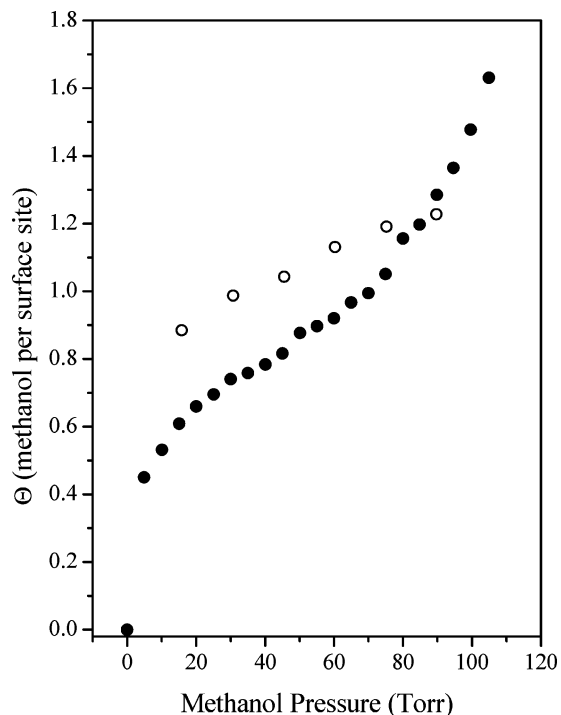
Figure 7. Adsorption isotherm of methanol on MgO(100) at room temperature. Data taken on ascending and descending pressures are given by closed and open circles, respectively.

Figure 8. Band center change with methanol coverages on MgO(100) at room temperature. Data taken on ascending and descending pressures are given by closed and open circles, respectively.

and O^{2-}. At pressures above 70 Torr, multilayers of methanol begin to form on the substrate. The crystal structure of MgO(100) has a cation interatomic distance of 2.8 Å,[42] which is a close match to the hydrogen-bonding oxygen interatomic distance of 3.0 Å[43] seen in hexagonal ice, and is most likely a distance that will allow the methanol molecule to interact with a surface ion and have the added stability of hydrogen bonding with a neighboring methanol molecule. Once all the surface sites have been filled, the impinging methanol molecule adsorbs onto this methanol monolayer, creating a second layer. Even at methanol pressures as high as 105 Torr, the methanol adlayer is minimal, with 1.63 layers being the maximum film thickness observed in this investigation. Once the methanol molecules begin three-dimensional growth on the surface, the hydrogen-bonding network in the adlayer loosens up and becomes more liquidlike.

This supposition most likely explains the shift in band center that begins at a pressure of 70 Torr, as seen in Figure 6. The correlation between coverage and band center is better revealed by Figure 8, which plots the band center of the adsorbed methanol hydroxyl stretch as a function of coverage. At coverages below one monolayer, the band is centered at 3260 cm^{-1}, but once the monolayer is complete and multilayer formation begins, the peak center begins to shift to the lower wavenumbers. As discussed earlier, the peak center seen for coverages of one monolayer and below closely resembles that of solid methanol. This tells us that, at coverages of one monolayer of methanol and below, the molecules are linked by a very rigid hydrogen-bonding network to the substrate. This monolayer seems to be quite stable as demonstrated by the coverage and peak center of a desorption series, represented by the open circles in Figures 6−8. At pressures as high as 90 Torr and as low as 15 Torr during a desorption series, the coverage remains fairly constant at one monolayer, and the band center falls within the submonolayer regime. Once multilayer growth begins, the hydrogen-bonding network becomes looser and more liquidlike as the adlayer grows in three dimensions.
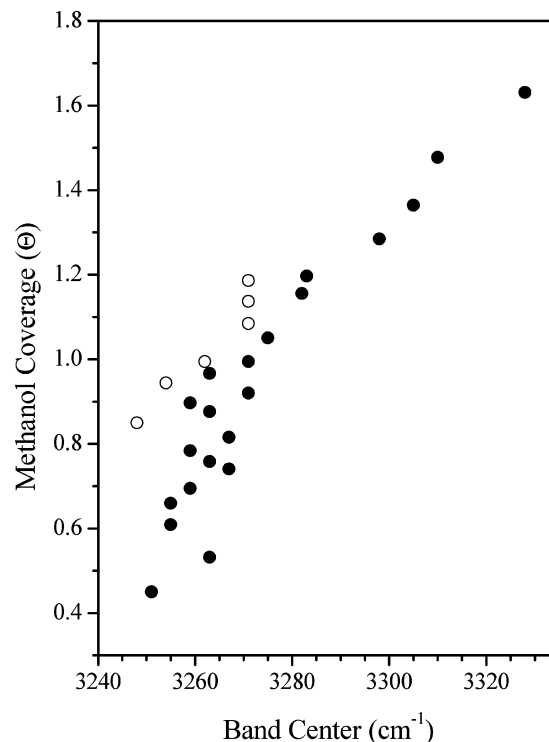
Conclusions

Methanol molecularly adsorbs to the magnesium oxide surface, forming reversible thin films at room temperature and under moderate-to-high methanol pressures. Film growth occurs by layers, with the completion of the monolayer before multilayer growth begins. At submonolayer coverages, the methanol forms a rigid, solidlike hydrogen-bonding network, while at multilayer coverages, the methanol adlayer has a liquidlike hydrogen-bonding network. The monolayer of methanol on MgO(100) is a fairly stable structure, as shown by the hysteresis seen during a full adsorption/desorption series. The maximum coverage obtained was less than two layers at a methanol vapor pressure of 105 Torr. All of the thin films discussed in this investigation are the result of the dynamic equilibrium occurring between methanol in the gas phase and a series of MgO(100) crystals.

References and Notes

(1) Onishi, H.; Egawa, C.; Aruga, T.; Iwasawa, Y. *Surf. Sci.* **1987**, *191*, 479.

(2) *Adsorption on Ordered Surfaces of Ionic Solids and Thin Films*; Freund, H.-J.; Umbach, E., Eds.; Springer-Verlag: Berlin, 1993.

(3) Noguera, C. *Physics and Chemistry at Oxide Surfaces*; Cambridge: Cambridge, 1996.

(4) Tench, A. J.; Giles, D.; Kibblewhite, J. F. J. *Trans. Faraday Soc.* **1971**, *67*, 854.

(5) Foyt, D. C.; White, J. M. *J. Catal.* **1977**, *47*, 260.

(6) Bensitel, M.; Saur, O.; Lavalley, J. C. *Mater. Chem. Phys.* **1991**, *28*, 309.

(7) Di Valentin, C.; Del Vitto, A.; Pacchioni, G.; Abbet, S.; Worz, A. S.; Judai, K.; Heiz, U. *J. Phys. Chem. B* **2002**, *106*, 11961.

(8) Gunster, J.; Liu, G.; Stultz, J.; Krischok, S.; Goodman, D. W. *J. Phys. Chem. B* **2000**, *104*, 5738.

(9) Goodman, D. W. *J. Vac. Sci. Technol., A* **1996**, *14*, 1526.

(10) Wu, M.-C.; Estrada, C. A.; Corneille, J. S.; Goodman, D. W. *J. Chem. Phys.* **1992**, *96*, 3892.

(11) Peng, X. D.; Barteau, M. A. *Langmuir* **1991**, *7*, 1426.

(12) Peng, X. D.; Barteau, M. A. *Catal. Lett.* **1992**, *12*, 245.

(13) Li, C.; Li, G.; Xin, Q. *J. Phys. Chem.* **1994**, *98*, 1933.

(14) Heidberg, J.; Redlich, B.; Wetter, D. *Ber. Bunsen-Ges. Phys. Chem.* **1995**, *99*, 1333.

(15) Liang, S. H. C.; Gay, I. D. *Langmuir* **1985**, *1*, 593.

(16) Branda, M. M.; Peralta, J. E.; Castellani, N. J.; Contreras, R. H. *Surf. Sci.* **2002**, *504*, 235.

(17) Branda, M. M.; Ferullo, R. M.; Belelli, N. J.; Castellani, N. J. *Surf. Sci.* **2003**, *527*, 89.

(18) Gunster, J.; Liu, J.; Stultz, J.; Goodman, D. W. *J. Chem. Phys.* **1999**, *110*, 2558.

(19) Foster, M.; Furse, M.; Passno, D. *Surf. Sci.* **2002**, *502−503*, 102.

(20) Foster, M.; Passno, D.; Rudberg, J. *J. Vac. Sci. Technol., A* **2004**, *22*, 1640.

(21) Simanouchi, T. *Tables of Molecular Vibrational Frequencies*; American Chemical Society: New York, 1972.

(22) Heidberg, J.; Redlich, B. *J. Electron Spectrosc. Relat. Phenom.* **1993**, *64/65*, 599.

(23) Kohno, Y.; Ishikawa, H.; Tanaka, T.; Funabiki, T.; Yoshida, S. *Phys. Chem. Chem. Phys.* **2001**, *3*, 1108.

(24) Carrier, X.; Doyle, C. S.; Kendelewicz, T.; Brown, G. E., Jr. *Surf. Rev. Lett.* **1999**, *6*, 1237.

(25) Peters, S. J.; Ewing, G. E. *J. Phys. Chem. B* **1997**, *101*, 10880.

(26) Dixon, J. R.; George, W. O.; Hossain, M. F.; Lewis, R.; Price, J. M. *J. Chem. Soc., Faraday Trans.* **1997**, *93*, 3611.

(27) Foster, M.; Ewing, G. E. *J. Chem. Phys.* **2000**, *112*, 6817.

(28) Al-Abadleh, H.; Grassian, V. H. *Langmuir* **2003**, *19*, 341.

(29) Al-Abadleh, H.; Grassian, V. H. *J. Phys. Chem. B* **2003**, *107*, 10829.

(30) Underwood, G. M.; Miller, T. M.; Grassian, V. H. *J. Phys. Chem. A* **1999**, *103*, 6184.

(31) Goodman, A. L.; Bernard, E. T.; Grassian, V. H. *J. Phys. Chem. A* **2001**, *105*, 6443.

(32) Falk, M.; Whalley, E. *J. Chem. Phys.* **1961**, *34*, 1554.

(33) Richardson, H. H.; Chang, H.-C.; Noda, C.; Ewing, G. E. *Surf. Sci.* **1989**, *216*, 93.

(34) Berg, O.; Ewing, G. E. *Surf. Sci.* **1989**, *220*, 207.

(35) Bertie, J. E.; Zhang, S. L.; Eysel, H. H.; Baluja, S.; Ahmed, M. K. *Appl. Spectrosc.* **1993**, *47*, 1100.

(36) Weis, D. D.; Ewing, G. E. *J. Geophys. Res. [Atmos.]* **1996**, *101*, 18709.

(37) Henrich, V. E.; Cox, P. A. *The Surface Science of Metal Oxides*; Cambridge University Press: Cambridge, 1996.

(38) Bertie, J. E.; Ahmed, M. K.; Eysel, H. H. *J. Phys. Chem.* **1989**, *93*, 2210.

(39) Downing, H. D.; Williams, D. *J. Geophys. Res.* **1975**, *80*, 1656.

(40) Warren, S. G. *Appl. Opt.* **1984**, *23*, 1206.

(41) Fujita, Y.; Ikawa, S.-I. *Chem. Phys. Lett.* **1989**, *159*, 184.

(42) *CRC Handbook of Chemistry and Physics,* 82nd ed.; Linde, D. R., Ed.; CRC Press: Boca Raton, FL, 2002; pp F167 and F169.

(43) Pimentel, G. C.; McClelland, A. L. *The Hydrogen Bond*; Reinhold: New York, 1960.